Retrieval of Soil Moisture and Vegetation Water Content Using SSM/I Data over a Corn and Soybean Region

JUN WEN, THOMAS J. JACKSON, RAJAT BINDLISH, AND ANN Y. HSU

Hydrology and Remote Sensing Laboratory, ARS, USDA, Beltsville, Maryland

Z. BOB SU

Wageningen University and Research Centre, ALTERRA Green World Research, Wageningen, Netherlands

(Manuscript received 21 July 2004, in final form 1 April 2005)

ABSTRACT

The potential for soil moisture and vegetation water content retrieval using Special Sensor Microwave Imager (SSM/I) brightness temperature over a corn and soybean field region was analyzed and assessed using datasets from the Soil Moisture Experiment 2002 (SMEX02). Soil moisture retrieval was performed using a dual-polarization 19.4-GHz data algorithm that requires the specification of two vegetation parameters—single scattering albedo and vegetation water content. Single scattering albedo was estimated using published values. A method for estimating the vegetation water content from the microwave polarization index using SSM/I 37.0-GHz data was developed for the region using extensive datasets developed as part of SMEX02. Analyses indicated that the sensitivity of the brightness temperature to soil moisture decreased as vegetation water content increased. However, there was evidence that SSM/I brightness temperatures changed in response to soil moisture increases resulting from rainfall during the later stages of crop growth. This was partly attributed to the lower soil and vegetation thermal temperatures that typically followed a rainfall. Comparisons between experimentally measured volumetric soil moisture and SSM/I-retrieved soil moisture indicated that soil moisture retrieval was feasible using SSM/I data, but the accuracy highly depended upon the levels of vegetation and atmospheric precipitable water; the standard error of estimate over the 3-week study period was 5.49%. The potential for using this approach on a larger scale was demonstrated by mapping the state of Iowa. Results of this investigation provide new insights on how one might operationally correct for vegetation effects using high-frequency microwave observations.

1. Introduction

Soil moisture remote sensing studies using passive microwave techniques conducted over several decades have clearly demonstrated the superiority of low-frequency sensors (Schmugge et al. 1974; Wang and Schmugge 1980; Jackson et al. 1995; Njoku and Li 1999; Paloscia et al. 2001). Global mapping has been limited by the high frequencies of the available satellite sensors. This has improved somewhat since the launch of the 10.7-GHz sensors on the Tropical Rainfall Measuring Mission (TRMM) and *Aqua* satellites (Njoku et al. 2003). The use of Advanced Microwave Scanning Radiometer (AMSR)-E observations at 6.9 GHz have been limited by the presence of radio frequency interference (RFI) (Li et al. 2004). The long-range outlook is good for soil moisture; three 1.4-GHz satellite sensors are planned for the future, the National Aeronautics and Space Administration (NASA) Hydros satellite (Entekhabi et al. 2004), the European Space Agency (ESA) Soil Moisture Ocean Salinity (SMOS) mission (Kerr et al. 2001), and the NASA Aquarius satellite (Koblinsky et al. 2003).

Many of the science goals that require soil moisture information also demand long-term records (Entekhabi et al. 2004). Because it will take many years to establish these with the future satellite systems, it is worthwhile to continue to explore what information can be obtained from available satellite systems with long records. The Special Sensor Microwave Imager (SSM/I) on the Defense Meteorological Satellite Program (DMSP)

Corresponding author address: Thomas J. Jackson, USDA, ARS, Hydrology and Remote Sensing Lab, 104 Bldg. 007, BARC-West, Beltsville, MD 20705.
E-mail: tjackson@hydrolab.arsusda.gov

platforms have collected global high-frequency microwave data for more than 17 yr since the first DMSP satellite was launched in 1987. Three SSM/I instruments are typically in operation at a given time and provide global multitemporal brightness temperature observations.

Several research efforts have confirmed that SSM/I 19.4-GHz brightness temperatures are somewhat sensitive to soil moisture and can sometimes be used for soil moisture retrieval under sparse vegetation conditions (Lakshmi 1998; Jackson 1997; Drusch et al. 2001; Jackson et al. 2002). A number of other soil moisture–related research efforts have been conducted using SSM/I brightness temperature data. Most of these studies were validated with a soil moisture surrogate. Basist et al. (2001) defined a soil wetness index using the SSM/I observations as a soil moisture indicator and compared it to local precipitation over several different climatic zones. The results showed that correlations between the soil wetness index and the Global Precipitation Climatology Project precipitation monthly anomalies were evident. Wang (1985) and Teng et al. (1993) analyzed relationships between the satellite-measured brightness temperature and the antecedent precipitation index (API) and found that relationships between the satellite observations and this index depended upon the geographic location and vegetation levels. It was concluded that API cannot be universally used to validate soil moisture retrieval algorithms. Vinnikov et al. (1999) indicated that the brightness temperature (<18 GHz) had utility as a soil moisture information source for the state of Illinois, except near the peak growth period of summer crops.

For the most part, these studies have involved sparsely vegetated or semiarid regions. For instance, the studies conducted in Oklahoma involved vegetation water contents of less than 0.5 kg m^{-2} (Jackson 1997). The influence of vegetation on microwave brightness temperature has not been sufficiently addressed in the past. One reason for this has been the paucity of ground vegetation measurements available. As part of the Soil Moisture Experiment 2002 (SMEX02), extensive soil moisture and vegetation water content datasets were developed over a corn and soybean region in the state of Iowa (Kustas et al. 2003; Jackson et al. 2004). These extensive datasets were used to analyze the potential for soil moisture and vegetation water content retrieval under significant levels of vegetation biomass using SSM/I data. In addition to these traditional analyses, the potential of soil moisture mapping over larger domains was explored using SSM/I data over the entire state of Iowa.

2. Soil moisture algorithm

The brightness temperatures measured by a satellite passive microwave radiometer integrate contributions from soil thermal temperature, soil moisture, surface roughness, and vegetation, as well as the atmosphere. Both vegetation and atmospheric contributions cannot be neglected at all SSM/I frequencies (19.4, 22.2, 37.0, and 85.0 GHz). Judge et al. (1997) have shown the effects of the atmospheric contribution using the *U.S. Standard Atmosphere*. The algorithm used here is founded on the following equation (Jackson et al. 2002):

$$T_{\mathrm{Bp}} = T_{\mathrm{au}} + L_{\mathrm{atm}}L_{\mathrm{veg}}^2(T_{\mathrm{ad}} + L_{\mathrm{atm}}T_{\mathrm{sky}})(1 - \varepsilon_p) + L_{\mathrm{atm}}L_{\mathrm{veg}}\varepsilon_p T_{\mathrm{soil}} + L_{\mathrm{atm}}T_{\mathrm{veg}}(1 - \omega_p)(1 - L_{\mathrm{veg}}) \times [1 + (1 - \varepsilon_p)L_{\mathrm{veg}}], \quad (1)$$

where T_{Bp} is the satellite-measured brightness temperature at p polarization, which refers to horizontal (h) or vertical (v) polarization; T_{au} and T_{ad} are the upwelling and downwelling atmospheric temperatures, respectively; T_{veg} and T_{soil} are the vegetation and soil thermal temperatures, respectively; L is the vegetation or atmospheric transmittance expressed as $L = \exp(-\tau\sec\theta)$, where θ is the incident angle of the observation; τ is the vegetation or atmospheric optical depth, which depends upon the vegetation or atmosphere extinction coefficient; ω_p is the vegetation single scattering albedo; ε_p is the soil emissivity at p polarization, which is related to soil water content and a soil surface roughness parameter; and T_{sky} is the cosmic brightness temperature.

Implementation of Eq. (1) into a soil moisture retrieval algorithm begins with the estimation of the upwelling and downwelling atmospheric temperatures computed from atmospheric transmittance and effective atmospheric temperature (Ulaby et al. 1982). Atmospheric transmittance and optical depth were estimated following Hiltbrunner (1998). The data that are required for these computations were derived from radiosonde observations made during SMEX02.

The cosmic brightness temperature T_{sky} is small at the SSM/I frequencies and is specified based upon published values (Hiltbrunner 1998). Another commonly used assumption that simplifies the solution is that $T_{\mathrm{veg}} = T_{\mathrm{soil}}$. The strength of this assumption will be dependent on the time of day. At times closer to the thermal crossover time (early morning), this is more reliable. Some studies, such as Hornbuckle and England (2004), have indicated that using an average of the air and soil temperatures might be better.

It was assumed that all vegetation parameters are

polarization independent. The 37-GHz observations are dominated by vegetation and, as a result, the underlying soil has almost no effect. At 19 GHz the soil makes a larger contribution to the signal. The implementation will require that single scattering albedo and optical depth be estimated independently. The formulation of Jackson and Schmugge (1991) was used to determine the optical depth from vegetation type and its current vegetation water content (VWC). In this approach a parameter b is assigned based upon land cover classification. The values assigned were derived from Jackson and Schmugge (1991), which were 0.162 for corn and 0.240 for soybean. The single scattering albedo was assigned a fixed value of 0.045 in this investigation.

Methods for estimating the VWC have been presented by Wen and Su (2004) using 10.7-GHz data, and by Jackson et al. (2004) using visible/infrared indices. Earlier investigators explored relationships between the Microwave Polarization Difference Index (MPDI), defined as $\text{MPDI} = 2(T_{\text{Bv}} - T_{\text{Bh}})/(T_{\text{Bv}} + T_{\text{Bh}})$, and vegetation parameters (Choudhury et al. 1987; Felde 1998). Koike et al. (2000) and Paloscia et al. (2001) have related the vegetation water content to the MPDI for a given vegetation type using the following expression:

$$\text{MPDI} = \frac{\text{MPDI}_0}{(1 + \text{VWC})^{\kappa/\cos\theta\sqrt{\lambda}}}, \tag{2}$$

where κ is an absorption coefficient that is dependent on the vegetation type with values ranging between 0.1 $m^{0.5}$ for sunflower and 0.4 $m^{0.5}$ for alfalfa (m is in meters) (Ulaby et al. 1986), MPDI_0 is the Microwave Polarization Difference Index for the bare soil surface, and λ is the sensor wavelength. In the current investigation the VWC will be estimated using a MPDI approach that will be developed for the study region.

After implementing all of the assumptions and deriving all of the inputs described above, Eq. (1) has two unknowns—soil emissivity and soil temperature. If we establish simultaneous equations for the horizontal and vertical brightness temperatures, it is then possible, through an iterative solution, to obtain estimates of both unknowns.

Soil moisture retrieval still requires one final step—the soil emissivity obtained by iteration contains the effect of surface roughness. This can be corrected by using the empirical model of Choudhury et al. (1979). Input parameters for this were based upon roughness measurements conducted during SMEX02. Surface heights were measured along 1-m transects in all study sites and used to compute the standard deviation, which is related to the roughness parameter. The standard deviations ranged from 0.51 to 1.52 cm with a mean of 0.94 cm (see information online at http://nsidc.org/data/amsr_validation/soil_moisture/smex02/).

The soil dielectric constant is then determined using the smooth surface soil emissivity and Fresnel equations. The soil moisture is finally estimated using soil texture information and a dielectric mixing model (Wang and Schmugge 1980; Schmugge 1980; Hallikainen et al. 1985).

3. Soil moisture experiment and SSM/I data

Several field experiments have been conducted in recent years that have attempted to provide appropriate soil moisture data for validation. Most of these experiments were conducted under low levels of vegetation water content (Jackson 1997; Jackson et al. 1999, 2002). To quantify the performance of these algorithms under higher levels of vegetation, a large-scale soil moisture field experiment was conducted over a corn and soybean region in the state of Iowa from 24 June to 12 July 2002 (Kustas et al. 2003). The geographic location of the SMEX02 study area and land cover patterns for the state of Iowa are shown in Fig. 1. The land cover patterns are similar throughout the state. Most of the area was dryland crop and pasture and was dominated by crops, 40% of which were soybean and 50% were corn. Three different spatial domains will be used in this investigation: the Walnut Creek watershed experimental area, the SMEX02 regional study area, and the state of Iowa.

Soil moisture sampling, as well as other relevant measurements, were conducted over the regional study area. More intensive sampling was conducted within the Walnut Creek watershed to support high-resolution remote sensing studies. Soil moisture observations were made at 3- and 6-cm depths using a combination of gravimetric and theta probe methods at 30 watershed sampling sites. At each site, 14 samples were averaged to obtain the field-averaged soil moisture.

Soil moisture observations were also made at 47 sampling sites within the regional study area. For any overpass, only a few SSM/I pixels (16–18) fell within the regional study area because of the large sensor footprint. To ensure that the ground measurements were representative of the SSM/I pixel footprint, the regional average of the experimentally measured daily soil moisture was used in this investigation.

During SMEX02, measurements of vegetation parameters, including the leaf area index and wet and dry biomass of corn and soybean, were made over the Walnut Creek watershed. The vegetation water content for corn ranged from 2.0 to 4.64 kg m^{-2}, and for soybean ranged from 0.2 to 0.83 kg m^{-2} (Jackson et al. 2004).

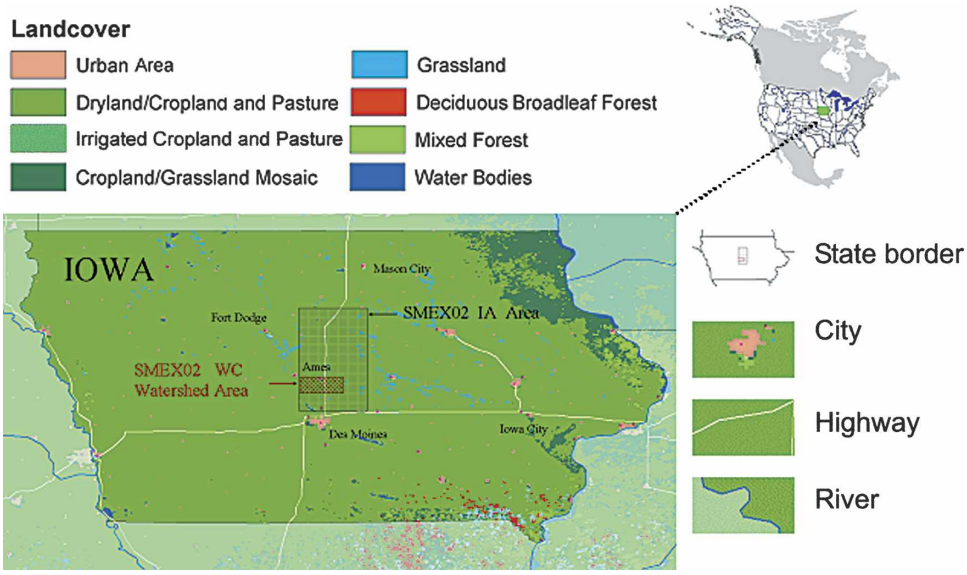

FIG. 1. Geographic location and land cover types of the soil moisture experimental area and the Iowa statewide area.

Fortunately for validation purposes, several rainfall events occurred during the experimental period, these events extended the dynamic range of the ground-measured volumetric soil moisture.

The SSM/I instruments on the DMSP satellites have measured the brightness temperature since 1987. The instrument is a conically scanning total power radiometer system operating at 19.4, 22.2, 37.0, and 85.5 GHz. All channels provide dual-polarization measurements, except that at 22.2 GHz, which has only vertical polarization. The basic specifications of the SSM/I instruments are summarized in Table 1. Three satellites with SSM/I instruments were available during the SMEX02 experimental period. For an individual satellite on a given day, it is possible to have coverage twice a day, however, it is also possible to have no coverage.

The SSM/I data we used were obtained from the National Oceanic and Atmospheric Administration (NOAA) Comprehensive Large Array-data Stewardship System (CLASS; see information online at http://www.saa.noaa.gov). Further processing of these data is necessary to convert antenna temperatures to brightness temperatures. All data for the region were extracted, processed, and provided to the National Snow and Ice Data Center (NSIDC) Distributed Active Archive Center (DAAC) for archival. Details of the data processing are included online (available at http://nsidc.org/data/amsr_validation/soil_moisture/smex02).

TABLE 1. The SSM/I platforms equatorial crossing times (local time zone) and spatial resolution.

Satellite	Date of operation	Ascending (LST)
DMSP F13	Mar 1996–present	1815
DMSP F14	Apr 1997–present	2021
DMSP F15	Dec 1999–present	2131
Frequencies (polarizations)		Spatial resolution (km)
19.4 GHz (vertical and horizontal)		69 × 43
22.2 GHz (vertical)		50 × 40
37.0 GHz (vertical and horizontal)		37 × 28
85.0 GHz (vertical and horizontal)		15 × 13

The previously discussed atmospheric correction scheme requires atmospheric water vapor profile information in order to calculate the precipitable water in the vertical atmosphere column. Radiosondes were launched a number of times a day during the experiment to characterize the boundary layer. The radiosondes were launched from a field located in the middle of the Walnut Creek watershed. Data from this location was used for both the SMEX02 area and a statewide study. The temperature and humidity radiosonde datasets collected during the experimental period were used for this purpose (http://nsidc.org/data/amsr_validation/soil_moisture/smex02). The soil texture data that were required in the dielectric mixing model were provided as ancillary datasets (Miller and White 1998).

4. Relationship between the MPDI and vegetation water content

The importance of the vegetation water content and optical depth was described above in the description of the soil moisture algorithm. Some investigators have

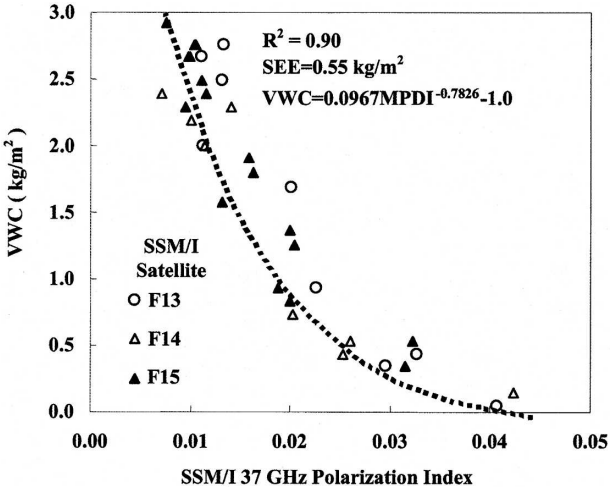

FIG. 2. The relationship between Landsat TM-derived crop vegetation water content and the SSM/I 37.0-GHz polarization index over the experimental area.

tried to derive this information from the MPDI, particularly using the 37-GHz data. Of particular relevance are studies reported by Owe et al. (2001) that used simulation modeling to establish relationships between the optical depth and MPDI. Here, the possibility of estimating VWC from the MPDI was explored.

The SMEX02 offered an unique opportunity to develop a VWC–MPDI relationship because of the extensive database and the wide range of VWC conditions. The VWC data used were generated as part of the investigation reported by Jackson et al. (2004). In that investigation, field-scale measurements were used with appropriate Landsat Thematic Mapper (TM) Normalized Difference Water Index (NDWI) datasets to establish corn- and soybean-specific VWC estimation equations specifically for SMEX02. Each Landsat image was then converted into a VWC database on a specific date. The multitemporal VWC databases were then interpolated to generate daily VWC datasets.

For each SSM/I 37-GHz MPDI observation, an average VWC within the footprint was derived using the data described above. The composite dataset is plotted in Fig. 2. From Fig. 2 we observed that the range of VWC that was available was large (~3 kg m^{-2}), which makes our analysis more robust. In addition, there is a clearly defined trend to the relationship that appears to be independent of the particular SSM/I satellite because the scatter is random about the trend line. As might be expected, the sensitivity of the MPDI to VWC appears to be highest at low levels of VWC and shows indications of saturation at very high levels of VWC. The sensitivity decreases significantly for VWC above 1.5 kg m^{-2}.

To develop a function to describe the relationship, we began by inverting Eq. (2) as follows:

$$\mathrm{VWC} = \frac{\mathrm{MPDI}_0^{\cos\theta\sqrt{\lambda/\kappa}}}{\mathrm{MPDI}^{\cos\theta\sqrt{\lambda/\kappa}}} - 1, \tag{3}$$

and then simplifying the form as follows:

$$\mathrm{VWC} = a_1\mathrm{MPDI}^{a_2} - 1. \tag{4}$$

The two coefficients a_1 and a_2 are expected to vary with the background soil, frequency, and vegetation type. For SMEX02, the observed VWC and MPDI values were used to optimize the coefficients through least squares regression. The values obtained were $a_1 = 0.0967$ and $a_2 = -0.7832$. The standard error of estimate of the resulting equation was 0.55 kg m^{-2}. It should be noted that in the previous discussion and throughout the paper, all error terms reported are in units of measurement for the variable.

5. Soil moisture retrieval validation

Because of the effects of the vegetation canopy, the sensitivity of SSM/I brightness temperature to soil moisture is typically low at high frequencies. The SMEX02 experimental period covered a portion of the crop-growing season during which time vegetation conditions ranged from low to dense. The SSM/I-measured brightness temperatures, averaged over the SMEX02 regional study area, are plotted separately as a time series for each SSM/I satellite in Fig. 3. Also shown in this figure is the daily precipitation time series. The regional daily precipitation was computed from the rain gauge data collected during the study period.

Figure 3 shows that the SSM/I 19.4-GHz brightness temperature responded to the rainfall events. Two major rainfall events and the periods that followed corresponded to low brightness temperatures. Brightness temperature gradually increased after these events. The rainfall-free dry period corresponded to high brightness temperature. These results, in particular, the late season event, suggested that SSM/I brightness temperatures retained some level of sensitivity to soil moisture throughout the entire SMEX02 period.

Although the SSM/I brightness temperature tended to decrease after rainfall, it must be noted that the microwave radiometer–measured brightness temperature also depends upon the soil thermal temperature, atmospheric effects, and vegetation water content. Interpreting satellite-based surface emissivity estimates is complicated by the fact that a decrease caused by increased soil moisture can be offset by an increase resulting from increased vegetation water content.

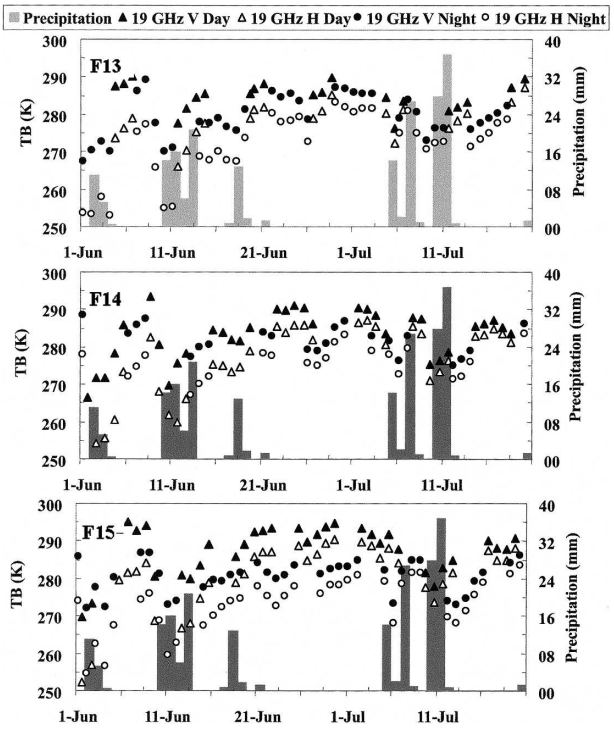

FIG. 3. Comparisons of the SSM/I 19.4-GHz brightness temperature and local precipitation over the experimental area: (top) DMSP F13, (middle) DMSP F14, and (bottom) DMSP F15.

SSM/I data over the study area, from both the ascending and descending orbits, from the three platforms (F13, F14, and F15) was extracted for the study period. There are typically from three to four SSM/I overpasses during a single day over the study area. Using the relationship between the SSM/I 37.0-GHz MPDI and the crop vegetation water content, the atmospheric correction method, SSM/I 19.4-GHz dual-polarized brightness temperatures, and the algorithm, the soil moisture was retrieved over the SMEX02 study area. Observed and predicted soil moisture values are presented in Fig. 4. Predicted values are also plotted as a time series in Fig. 5. In addition to the retrievals for each individual satellite overpass on a given day, the daily averaged estimated soil moisture was computed by averaging the estimated soil moisture from all of the satellite observations.

The SSM/I-based soil moisture is generally consistent with the ground measurements, except on 9, 10, 11 and 12 July 2002. Over the duration of the experiment, the vegetation grew to significantly high levels (VWC values of corn of ~5 kg m^{-2} and of soybean of ~1 kg m^{-2}). With the increase in vegetation, the soil moisture signal is significantly attenuated. Also, there was a significant amount of precipitation on 10–11 July over the entire study area (~50 mm). The occurrence of

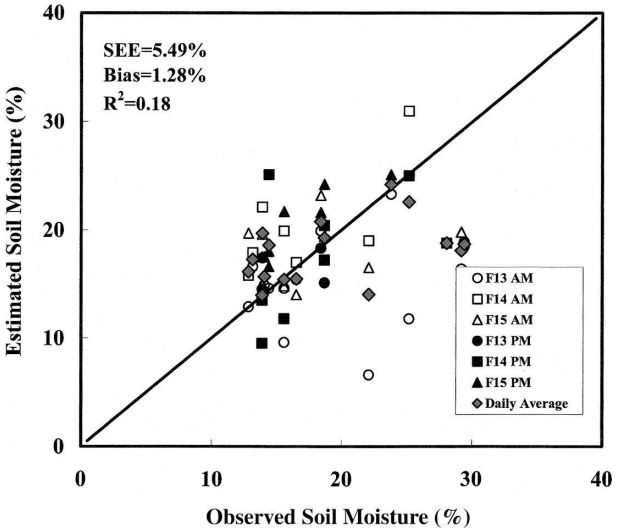

FIG. 4. Comparison of the SSM/I-based soil moisture and the SMEX02 ground-measured regional-averaged volumetric soil moisture.

precipitation also resulted in an increase in the levels of atmospheric water vapor for 10–11 July measured by the radiosondes (35–45 mm as compared to <25 mm before 10 July). Such an increase in atmospheric water vapor would also impact our ability to retrieve soil moisture. As a result, even though there were multiple satellite overpasses on 10, 11, and 12 July, only two overpass observations on 10 and 11 July and one on 12 July resulted in a soil moisture estimate. The algorithm was unable to converge for the other observations.

The increase in vegetation and atmospheric water vapor increases the attenuation of the microwave emissions. As the vegetation water content increases the

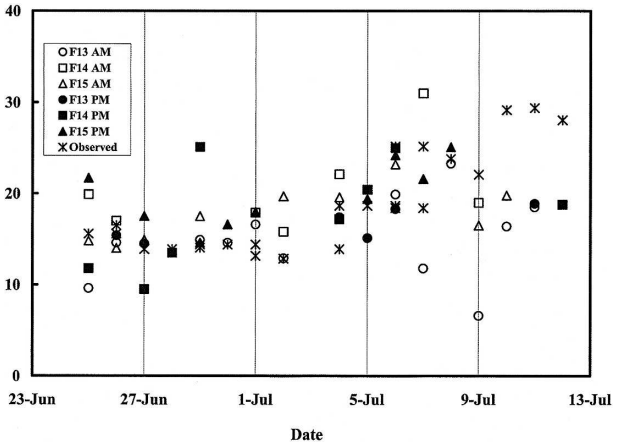

FIG. 5. Time series of SSM/I-predicted soil moisture for SMEX02.

sensitivity of the spaceborne brightness temperatures to soil emissivity reduces. The decrease in soil emissivity results in a decrease in soil moisture sensitivity. The standard deviation of the estimated soil moisture increased with the increase of the vegetation water content. This decrease in soil moisture sensitivity leads to poor convergence. These factors may explain the difference between the ground-measured and satellite-retrieved soil moistures. The standard error of estimate (SEE) for the retrieved soil moisture was 5.49% in this study. Previous SSM/I soil moisture retrievals over grassland have reported a SEE of 5.14%–5.75% (Jackson 1997; Jackson et al. 2002).

Errors in the retrieved soil moisture might also be related to the inherent limitations involved in estimating the soil surface roughness parameter, even with field measurements (Choudhury et al. 1979), as well as the accuracy of the atmospheric and vegetation correction methods. Errors associated with the effects of vegetation and atmosphere were previously discussed under the assumption that the other parameters did not contribute to significant errors in the soil moisture retrieval (Wen et al. 2003). To analyze soil moisture variation that might be caused by uncertainty in a specific parameter, the first derivatives were computed for the soil moisture retrieval algorithm. For a specified parameter, if other parameters are held constant, the soil moisture variation caused by the uncertainty of this specified parameter can be used to understand the potential sources of error in the retrieved soil moisture. Computations show that a 2.0-mm uncertainty in the precipitable water used in the atmosphere results in a 0.5%–1.1% error in the estimated soil moisture; a 0.2 kg m^{-2} uncertainty in the vegetation water content when the VWC is 1.5 kg m^{-2} can cause a 1.5% error in soil moisture, and the same uncertainty when the VWC is 2.0 kg m^{-2} will cause a 6.4% error in the estimated soil moisture. The VWC values used in Fig. 3 represent the regional corn and soybean mixture. When the vegetation water content was greater than 3.0 kg m^{-2}, the error increased rapidly (Wen et al. 2003).

SSM/I has a footprint resolution of 69 km $\times$ 43 km at 19.4 GHz. Linear scaling was assumed while aggregating the ancillary datasets to the SSM/I resolution. Studies have shown the effect of scaling and linear aggregation on the soil moisture estimates (Jackson 2001). This is especially true when aggregating over heterogeneous areas (the SMEX02 study area has a mixture of corn and soybean areas). The coarse resolution of the SSM/I footprints, the nonlinearity in the radiative transfer, and the antenna gain may all lead to errors in soil moisture estimates. The linear averaging of soil moisture over heterogeneous areas can introduce significant differences when compared to SSM/I observations (up to 17% volumetric soil moisture) (Drusch et al. 1999). The soil moisture estimates derived from the SSM/I data were between 10% and 20% at the start of the experiment on 25 June. The estimates stayed in this range for the first half of the experiment until 3 July. These estimates are consistent with the ground observations. The estimated soil moisture increased after the precipitation event of 4 July. As discussed earlier, the estimated soil moisture did not compare well with the observations after 9 July. The SSM/I soil moisture algorithm was not able to correctly estimate the high soil moisture conditions observed after the 10–11 July precipitation event.

6. Statewide soil moisture mapping

As an example of the potential of soil moisture retrieval over even larger regions, we retrieved soil moisture for the entire state of Iowa using the algorithm described above. Because the vegetation, soils, and climate are similar throughout the state, the extension should be valid. Figure 6 illustrates the results with four selected SSM/I-based volumetric soil moisture regional distributions. Statewide rainfall data collected over the duration of SMEX02 was interpolated to produce precipitation images. Daily precipitation data from 176 weather stations located in the state of Iowa were used for this analysis. For comparison, we have also included color-scale images of the antecedent daily precipitation for the observation date, as well as two preceding days. The state of Iowa received no rainfall on 25 June, and only scattered showers on 26 and 27 June. This resulted in moderately dry conditions at the beginning of the exercise (SSM/I-estimated soil moisture was 10%–15%). This was followed by a period with no observed precipitation, which resulted in very dry conditions on 1 July, with soil moisture estimates of 5%–10%. The dry period was followed by scattered precipitation on 5–7 July (rainfall observations of 25–30 mm over central Iowa). The estimated soil moisture was significantly higher over the entire area (20%–30% estimates). The heavy rains on 10–11 July (some areas recorded precipitation amounts over 50 mm during this period) resulted in very wet conditions on 11 July (soil moisture estimates of 30%–40%). These estimates are consistent with the observations in the SMEX02 experimental area.

In general, the retrieved soil moisture distributions in Fig. 6 reflect regional soil moisture patterns that we would expect based upon the rainfall distributions. During the driest period of SMEX02, that is, 1 July 2002, the retrieved soil moisture values were also low.

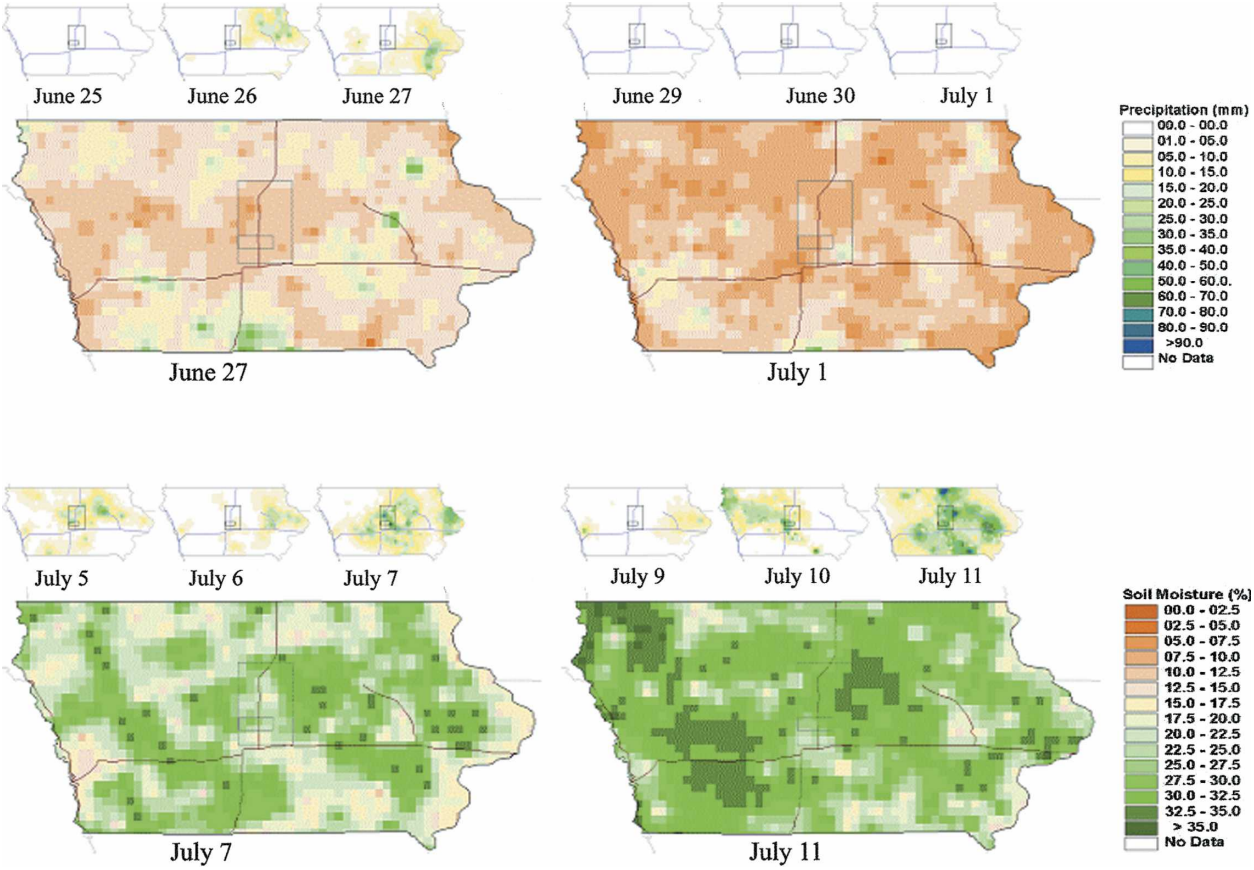

FIG. 6. The Iowa statewide regional soil moisture distributions on 27 Jun, and 1, 7, and 11 Jul 2002 (large maps), and the corresponding daily antecedent precipitation (smaller maps).

There was precipitation from 7 to 11 July, and the retrieved soil moisture values were high on these 2 days. These results demonstrate that the SSM/I-based approach presented in this study is capable of reliably mapping large-scale soil moisture under low levels of vegetation cover with VWC up to 2 kg m^{-2}. Jackson et al. (2002) showed that it was possible to obtain SSM/I-based soil moisture with error levels of 5% over less dense vegetation conditions (VWC < 1.5 kg m^{-2}).

7. Conclusions

The ability of an SSM/I-based soil moisture algorithm under significant levels of vegetation was evaluated. A unique database from a large-scale field experiment (SMEX02) allowed us to develop and test a method for estimating the vegetation water content from the SSM/I 37.0-GHz Microwave Polarization Difference Index. The sensitivity of this function decreased as the VWC increased. Brightness temperature analyses showed that the crops in Iowa have an obvious and expected effect on the SSM/I brightness temperature. The vegetation reduced the sensitivity of the brightness temperature to soil moisture, especially at high-levels of vegetation water content. However, SSM/I 19.4-GHz brightness temperatures showed some responses to the antecedent precipitation and tended to decrease as the soil moisture increased during the SMEX02 experimental period, which is the expected relationship. After specifying all input and ancillary datasets, the SSM/I 19.4-GHz dual-polarized brightness temperature and the proposed soil moisture algorithm were used to retrieve soil moisture over the SMEX02 regional study area. A 5.49% standard error of estimate was observed for volumetric soil moisture for the entire study period. A statewide extension of the algorithm produced soil moisture patterns that were credible when compared to the daily antecedent precipitation. This study concludes that soil moisture retrieval is possible using the SSM/I observations, but the accuracy is limited under high-level vegetation and cloud conditions. Results of this investigation provide new insights on how we might operationally correct for vegetation effects using high-frequency microwave observations.

Acknowledgments. This work was supported in part by the NASA EOS *Aqua* Calibration/Validation and Terrestrial Hydrology Programs. The contributions from the other SMEX02 teams are gratefully acknowledged.

REFERENCES

Basist, A., C. Williams, N. C. Grody, T. F. Ross, S. Shen, A. T. C. Chang, R. Ferraro, and M. J. Menne, 2001: Using the Special Sensor Microwave Imager to monitor surface wetness. *J. Hydrometer.,* **2,** 297–308.

Choudhury, B. J., T. J. Schmugge, A. Chang, and R. W. Newton, 1979: Effect of surface roughness on microwave emission from soils. *J. Geophys. Res.,* **84,** 5699–5706.

——, C. J. Tucker, R. E. Golus, and W. W. Newcomb, 1987: Monitoring vegetation using Nimbus-7 scanning multichannel microwave radiometer data. *Int. J. Remote Sens.,* **8,** 533–538.

Drusch, M., E. F. Wood, and R. Lindau, 1999: The impact of SSM/I antenna gain function on land surface parameter retrieval. *Geophys. Res. Lett.,* **26,** 3481–3484.

——, ——, and T. J. Jackson, 2001: Vegetative and atmospheric corrections for the soil moisture retrieval from passive microwave remote sensing data: Results from the Southern Great Plains hydrology experiment 1997. *J. Hydrometer.,* **2,** 181–192.

Entekhabi, D., and Coauthors, 2004: The Hydrosphere State (Hydros) mission: An Earth System Pathfinder for global mapping of soil moisture and land freeze/thaw. *IEEE Trans. Geosci. Remote Sens.,* **42,** 2184–2195.

Felde, G. W., 1998: The effect of soil moisture on the 37GHz microwave polarization difference index (MPDI). *Int. J. Remote Sens.,* **19,** 1055–1078.

Hallikainen, M. T., F. T. Ulaby, M. C. Dobson, M. A. El-Rayes, and L. K. Wu, 1985: Microwave dielectric behavior of wet soil. Part I: Empirical models and experimental observations. *IEEE Trans. Geosci. Remote Sens.,* **23,** 25–34.

Hiltbrunner, D., 1998: Land surface temperature and microwave emissivity from SSM/I data. Ph.D. dissertation, University of Bern, 176 pp.

Hornbuckle, B. K., and A. W. England, 2004: Modeling 1.4 GHz land surface brightness: What measure of vegetation temperature should be used? *Proc. of the Int. Geoscience and Remote Sensing Symp*., Vol. I, Anchorage, AK, IEEE, Catalog No. 04CH37612C, 344–347.

Jackson, T. J., 1997: Soil moisture estimation using special satellite microwave/imager satellite data over a grassland region. *Water Resour. Res.,* **33,** 1475–1484.

——, 2001: Multiple resolution analysis of L band brightness temperature for soil moisture. *IEEE Trans. Geosci. Remote Sens.,* **39,** 151–164.

——, and T. J. Schmugge, 1991: Vegetation on the microwave emission of soil. *Remote Sens. Environ.,* **36,** 203–212.

——, D. M. Le Vine, C. T. Swift, T. J. Schmugge, and F. R. Schiebe, 1995: Large area mapping of soil moisture using the ESTAR passive microwave radiometer in Washita'92. *Remote Sens. Environ.,* **53,** 27–37.

——, ——, A. Y. Hsu, A. Oldak, P. J. Starks, C. T. Swift, J. D. Isham, and M. Haken, 1999: Soil moisture mapping at regional scales using microwave radiometry: The Southern Great Plains Hydrology Experiment. *IEEE Trans. Geosci. Remote Sens.,* **37,** 2136–2151.

——, A. Y. Hsu, and P. E. O'Neill, 2002: Surface soil moisture retrieval and mapping using high-frequency microwave satellite observations in the Southern Great Plains. *J. Hydrometer.,* **3,** 688–699.

——, D. Y. Chen, M. Cosh, F. Q. Li, M. Anderson, C. Walthall, P. Doriaswamy, and E. R. Hunt, 2004: Vegetation water content mapping using Landsat data derived normalized difference water index for corn and soybeans. *Remote Sens. Environ.,* **92,** 475–482.

Judge, J., J. F. Galantowicz, A. W. England, and P. Dahl, 1997: Freeze/thaw classification for prairie soils using SSM/I radiobrightnesses. *IEEE Trans. Geosci. Remote Sens.,* **35,** 827–832.

Kerr, Y. H., P. Waldteufel, J. P. Wigneron, J. M. Martinuzzi, J. Font, and M. Berger, 2001: Soil moisture retrieval from space: The Soil Moisture Ocean Salinity (SMOS) mission. *IEEE Trans. Geosci. Remote Sens.,* **39,** 1729–1735.

Koblinsky, C. J., P. Hildebrand, D. LeVine, F. Pellerano, Y. Chao, W. Wilson, S. Yueh, and G. Lagerloef, 2003: Sea surface salinity from space: Science goals and measurement approach. *Radio Sci.,* **38,** 8064, doi:10.1029/2001RS002584.

Koike, T., E. G. Njoku, T. J. Jackson, and S. Paloscia, 2000: Soil moisture algorithm development and validation for the ADEOS/AMSR. *Proc. of the Int. Geoscience and Remote Sensing Symp.,* Vol. III, Honolulu, HI, IEEE, 1253–1255.

Kustas, W. P., T. J. Jackson, J. H. Prueger, J. L. Hatfield, and M. C. Anderson, 2003: Remote sensing field experiments evaluate retrieval algorithms and land-atmosphere modeling. *Eos, Trans. Amer. Geophys. Union,* **84,** 491–493.

Lakshmi, V., 1998: Special sensor microwave imager data in field experiments: FIFE-1987. *Int. J. Remote Sens.,* **19,** 481–505.

Li, L., E. G. Njoku, E. Im, P. Chang, and K. S. Germain, 2004: A preliminary survey of radio-frequency interference over the U.S. in Aqua AMSR-E data. *IEEE Trans. Geosci. Remote Sens.,* **42,** 380–390.

Miller, D. A., and R. A. White, 1998: A conterminous United States multi-layer soil characteristics data set for regional climate and hydrology modeling. Earth Interactions **2**. [Available online at http://EarthInteractions.org.]

Njoku, E. G., and L. Li, 1999: Retrieval of land surface parameters using passive microwave measurements at 6 to 18 GHz. *IEEE Trans. Geosci. Remote Sens.,* **37,** 79–93.

——, T. J. Jackson, V. Lakshmi, T. K. Chan, and S. V. Nghiem, 2003: Soil moisture retrieval from AMSR-E. *IEEE Trans. Geosci. Remote Sens.,* **41,** 215–229.

Owe, M., R. de Jeu, and J. Walker, 2001: A methodology for surface soil moisture and vegetation optical depth retrieval using the microwave polarization difference index. *IEEE Trans. Geosci. Remote Sens.,* **39,** 1643–1654.

Paloscia, S., G. Macelloni, E. Santi, and T. Koike, 2001: A multifrequency algorithm for the retrieval of soil moisture on a large scale using microwave data from SMMR and SSM/I. *IEEE Trans. Geosci. Remote Sens.,* **39,** 1655–1661.

Schmugge, T. J., 1980: Effect of texture on microwave emission from soil. *IEEE Trans. Geosci. Remote Sens.,* **18,** 353–361.

——, P. Gloerson, T. Wilheit, and F. Geiger, 1974: Remote sensing of soil moisture with microwave radiometer. *J. Geophys. Res.,* **79,** 317–323.

Teng, W. L., J. R. Wang, and P. C. Doraiswamy, 1993: Relationship between satellite microwave radiometric data, antecedent precipitation index, and regional soil moisture. *Int. J. Remote Sens.,* **14,** 2483–2500.

Ulaby, F. T., R. K. Moore, and A. K. Fung, 1982: *Radar Remote Sensing and Emission Theory*. Vol. II, *Microwave Remote Sensing: Active and Passive,* Addison-Wesley Publishing, 608 pp.

——, ——, and ——, 1986: *From Theory to Application*. Vol. III, *Microwave Remote Sensing: Active and Passive*, Addison-Wesley Publishing, 1098 pp.

Vinnikov, K. Y., A. Robock, S. Qiu, J. K. Entin, M. Owe, B. J. Choudhury, S. E. Hollinger, and E. G. Njoku, 1999: Satellite remote sensing of soil moisture in Illinois, United States. *J. Geophys. Res.,* **104** (D4), 4145–4168.

Wang, J. R., 1985: Effect of vegetation on soil moisture sensing from an orbiting radiometer. *Remote Sens. Environ.,* **17,** 141–151.

——, and T. J. Schmugge, 1980: An empirical model for the complex dielectric permittivity of soils as function of water content. *IEEE Trans. Geosci. Remote Sens.,* **18,** 288–302.

Wen, J., and Z. B. Su, 2004: An analytical algorithm on the determination of LAI from TRRM/TMI data. *Int. J. Remote Sens.,* **25,** 1223–1234.

——, ——, and Y. M. Ma, 2003: Determination of land surface temperature and soil moisture from Tropical Rainfall Measuring Mission/Microwave Imager remote sensing data. *J. Geophys. Res.,* **108,** 4038, doi:10.1029/2002JD002176.